

# KNOWDATA: KNOWLEDGE-ENABLED DATA GENERATION FOR IMPROVING MULTIMODAL MODELS

**Anonymous authors**

Paper under double-blind review

## ABSTRACT

In this paper, we introduce a novel framework to enhance the quality of synthetic image-text pairs for multimodal models such as CLIP. Our approach, named KnowData, integrates real-world knowledge explicitly into the generation of text descriptions. It combines structured knowledge from knowledge graphs like ConceptNet and unstructured knowledge extracted from Wikipedia, to ensure that the generated text descriptions are both contextually rich and accurately reflective of real-world knowledge. Additionally, we leverage Large Language Models for the expansion, summarization, and refinement of the text descriptions to ensure their coherence. These enriched texts are subsequently used to generate images through advanced text-to-image models like Stable Diffusion and DALLE-3. CLIP models are then fine-tuned with these synthetic data for downstream zero-shot image classification tasks. Our experiments across 9 datasets demonstrate that CLIP models fine-tuned with our knowledge-guided synthetic datasets outperform 6 state-of-the-art zero-shot CLIP methods (e.g., +11.23% on DTD and +4% on EuroSAT based on ViT-B/16 model; +11.47% on CIFAR-100 and +7.99% on DTD based on ResNet-50 model). These results showcase the improved out-of-distribution robustness and adaptability of KnowData across a diverse set of data domains. We further verify the design of KnowData through ablation studies, revealing that the integration of knowledge in the text descriptions contributes to the reliability, diversity, and detail orientation of the synthetic images, thereby offering better data scaling laws for CLIP zero-shot image classification performance.

## 1 INTRODUCTION

Multimodal learning, particularly in image-text models such as Contrastive Language-Image Pre-training (CLIP) (Radford et al., 2021) has witnessed transformative advancements in recent years. These models excel in understanding and correlating the nuances of visual and textual data, leading to applications in a wide range of domains. Despite their versatility, a critical aspect of their development hinges on the quality and relevance of their training datasets. Traditional dataset collection methods, predominantly based on extensive web crawling, could compromise on the contextual richness and accuracy of text-image pairs due to the inclusion of noisy data on the internet (Feng et al., 2024).

To fill in this gap, there have been several approaches proposed to improve the quality of image-text pairs as training or fine-tuning data. For instance, to enhance data quality when building the powerful DALLE-3 model, Betker et al. (2023) trained a bespoke image captioner to recaption the image dataset. Also, it has been shown that merely enlarging the training data size or combining multiple sources does not necessarily lead to better multimodal models, while the data quality plays the key role (Nguyen et al., 2022; Fang et al., 2022). Existing studies mainly focus on using the implicit knowledge in language models to improve the text quality of image-text pairs (He et al., 2023; Shipard et al., 2023), which may lack factuality and diversity (Betker et al., 2023). In our work, we explore the question: *Can we explicitly integrate real-world knowledge to improve the quality of image-text pairs and further improve the performance and robustness of multimodal models?*

To explicitly leverage real-world knowledge to improve data quality, we propose a novel data generation framework KnowData (shown in Figure 1), which introduces a knowledge-guided approach to generate text-image pairs with multiple knowledge sources, including large-scale knowledge graphs,

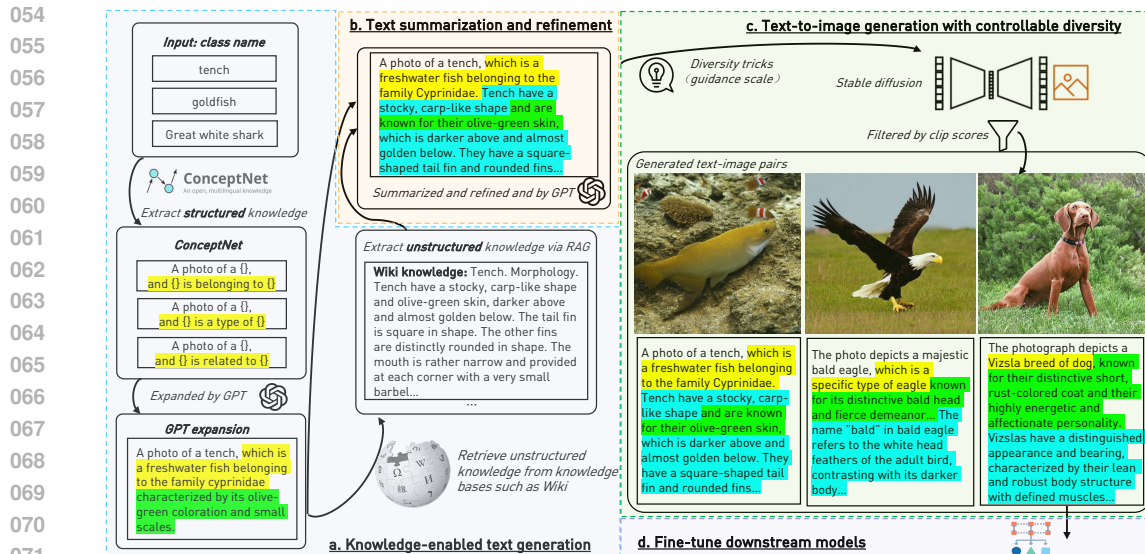


Figure 1: The proposed KnowData framework consists of four components: a) knowledge-enabled description generation, b) description summarization and refinement, c) image generation with controlled diversity, and d) downstream model fine-tuning. Here yellow texts indicate structured knowledge added through the knowledge graph (e.g., ConceptNet), blue texts signifies unstructured knowledge augmented from knowledge stores (e.g., Wikipedia) through RAG, and green texts represent knowledge expanded through LLMs.

Wikipedia knowledge stores, and Large Language Models (LLMs). In particular, (1) we first leverage the *structured* knowledge from knowledge graphs such as ConceptNet (Speer et al., 2017) to generate text that explicitly reflects basic object properties and relations (e.g., “Vizsla is related to dog”). (2) Furthermore, we use LLM to *expand* the structured knowledge sentences for more coherent descriptions with supplementary details. (3) We then integrate the *unstructured* knowledge extracted from external knowledge stores. We build a Retrieval Augmented Generation (RAG) pipeline to extract related knowledge and description from Wikipedia (e.g., “The Hungarian Vizsla is a short-coated hunting dog...The nose of the Vizsla will always have a reddish color that blends with the coat color.”). (4) We then pass the text generated based on structured and unstructured knowledge to LLM to *refine and summarize* it, which leads to texts following the real-world text data distribution while containing multi-source knowledge. (5) Next, we use text-to-image models like Stable Diffusion (Rombach et al., 2022) or DALLE-3 (Betker et al., 2023) to generate images based on the refined texts. For each text input, we integrate different diversity constraints to generate multiple images, and select the high-quality pairs based on certain criteria such as CLIP scores (Radford et al., 2021). (6) Finally, we leverage our generated data to fine-tune the multimodal models. By integrating contextual and domain-specific insights into the text generation process and diversity tricks into the image generation phase, we aim to create high-quality training datasets, thereby enhancing the learning efficacy and application potential of **multimodal models** like CLIP.

Our extensive experiments demonstrate that CLIP models fine-tuned with our knowledge-guided, synthesized dataset outperform those trained with state-of-the-art (SOTA) **data generation approaches** (He et al., 2023; Shipard et al., 2023) and other **zero-shot techniques** (Allingham et al., 2023; Menon & Vondrick, 2023; Ge et al., 2023). We systematically evaluate KnowData across 9 datasets, highlighting its robustness and adaptability in various data domains. For instance, on ViT-B, we achieve performance improvements of 11.23% on the DTD dataset and 4% on the EuroSAT dataset compared to the SOTA. On RN50, we achieved improvements of 11.47% on the CIFAR-100 and 7.99% on DTD. Furthermore, our ablation studies show that (1) by gradually adding more knowledge sources for text descriptions, KnowData produces synthetic images with better reliability, diversity, and accurate details; (2) KnowData benefits from stronger text-to-image generators; (3) KnowData enables better data scaling law; (4) diversity in text knowledge and diversity in images both matter.

Our findings highlight the effectiveness of knowledge-infused synthetic data in enhancing CLIP models’ generalization capabilities, suggesting a need to reevaluate dataset design strategies in

multimodal learning. This study aims to **present a new data generation pipeline** and ignite further research into knowledge-guided approaches for multimodal learning.

## 2 RELATED WORK

To demonstrate the capability of our knowledge-enabled data generation, we primarily evaluate our generated data on improving CLIP zero-shot classification performance (i.e., without using real data). Existing approaches to improving CLIP’s zero-shot performance include *enhancing the per-class text embedding with additional content*, and *fine-tuning CLIP model with synthetic data*.

**Enhancing the per-class text embedding with additional content.** For vision-language models like CLIP, the classification outcome is determined by finding the class label whose text embedding is most similar to the image embedding. Enhancing text descriptions about class labels can improve CLIP classification performance. For example, [Allingham et al. \(2023\)](#) use LLMs to generate additional text prompt templates and perform weighted selection among these templates, while [Menon & Vondrick \(2023\)](#) uses LLMs to derive descriptions for class names to obtain text embeddings. [Ge et al. \(2023\)](#) supplements class names with hierarchical knowledge from WordNet to enhance text embeddings. Despite leveraging knowledge, these methods lack systematic, explicit injection of diverse and accurate knowledge, which may result in irrelevant or false information generated from LLMs. Our approach uses multiple knowledge sources to ensure both diversity and accuracy. Moreover, the aforementioned methods are limited to manual adjustments at the text embedding level. In contrast, we use knowledge to generate synthetic text-image pairs and then fine-tune the model, which can provide more flexible and thorough model adjustment.

**Fine-tuning models with synthetic data.** Existing studies employ various generation tricks for diffusion models to enhance the diversity and quality of generated images and then finetune the CLIP model, but they fail to effectively incorporate the relevant knowledge of the class itself into the generation process ([Shipard et al., 2023](#); [Sarıyıldız et al., 2023](#)). [He et al. \(2023\)](#) employs a word-to-sentence T5 model to enrich prompts and generate images, but this approach merely randomizes class expressions without systematically enriching class-related knowledge. Other studies, such as [Bansal & Grover \(2023\)](#) and [Trabucco et al. \(2023\)](#), use synthetic data for data augmentation, and [Fan et al. \(2023\)](#) explore the scaling laws of synthetic images for image classification tasks, without enhancing the quality of generated data. In contrast, our knowledge-enabled data generation framework produces higher-quality text descriptions and synthetic images with more detailed features, enhancing CLIP zero-shot performance on downstream tasks.

**Text-to-Image Diffusion Models.** Diffusion models have significantly advanced text-to-image generation by producing high-quality images from textual descriptions ([Sohl-Dickstein et al., 2015](#); [Ho et al., 2020](#); [Nichol & Dhariwal, 2021](#)). Notable models like Stable Diffusion ([Rombach et al., 2022](#)), Imagen ([Saharia et al., 2022](#)), GLIDE ([Nichol & Dhariwal, 2021](#)), and DALLE-3 ([Betker et al., 2023](#)) have demonstrated impressive capabilities in this domain. However, these models often lack explicit knowledge utilization, leading to synthetic images that may miss certain detailed features. This gap motivates our exploration of knowledge-enabled synthetic data generation.

## 3 KNOWDATA

In this section, we describe how we generate knowledge-enabled texts (Section 3.1 and Section 3.2), create diverse images based on these texts by adding image diversity constraints (Section 3.3), and utilize the synthetic data to fine-tune the downstream models (Section 3.4).

### 3.1 KNOWLEDGE-ENABLED DESCRIPTION GENERATION

Our knowledge-enabled description generation pipeline is designed to produce high-quality prompts from a given class name. Subsequently, these prompts can be utilized by text-to-image diffusion models to generate superior images. Our pipeline integrates diverse types of knowledge from various sources. Specifically, we incorporate structured knowledge derived from large-scale knowledge graphs, and unstructured knowledge from external knowledge stores via the Retrieval Augmented Generation (RAG) framework and LLM, thereby enriching the details of the generated text.

Formally, let  $\{c_1, \dots, c_K\}$  be a list of targeted classes names, where  $K$  is the total number of classes. We generally use  $x$  to denote the class description prompt used for image generation within the

pipeline. The naive base prompt  $x_i^{base}$  can be “A photo of  $c_i$ ” for each class  $c_i$ , where  $i \in [K]$ . Next, we will elaborate on how we improve over the base prompt by incorporating diverse knowledge.

**Extracting unstructured knowledge from knowledge graphs.** Knowledge graphs are advanced data structures that map out the connections between various entities, such as objects, people, places, and concepts, to organize and integrate structured knowledge from multiple sources (Hogan et al., 2021). Considering their comprehensive and interconnected representation of information, we first supplement the classes with commonsense knowledge based on external knowledge graphs. The use of external knowledge graphs does not rely on additional models and, most importantly, ensures the *correctness and broadness* of the integrated knowledge. In this work, we choose ConceptNet (Speer et al., 2017) for structured knowledge extraction. Unlike some other knowledge graphs, such as ATOMIC (Hwang et al., 2021) that provides commonsense knowledge around human events, ConceptNet is more focused on encyclopedic knowledge. This aligns well with the natural image datasets we plan to evaluate, such as ImageNet.

Specifically, each node in ConceptNet represents one entity (e.g., object), and the edge represents the relations between entities. We query the ConceptNet API with each class name  $c_i$  as input, which will return triplets of {head, relation, tail} where  $c_i$  appears either in the head or tail. We consider 18 relations that may benefit our image recognition task, such as “RelatedTo”, “IsA”, “PartOf”, “LocatedNear”, and then only select triplets describing those relations. We then create templates to convert these relations into more understandable sentences, e.g., replacing “{ } RelatedTo { }” with “{ } is related to { }”. We defer the complete list of 18 chosen relations and corresponding alternative templates to Appendix C. Then we concatenate the base prompt  $x_i^{base}$  with the ConceptNet sentence (e.g., “A photo of  $c_i$ , and  $c_i$  is related to { }”) to obtain our description in the knowledge graph enhancement stage of KnowData. We retrieve  $N$  such structured knowledge descriptions for each class  $c_i$ , denoted as  $x_{i,j}^{kg} = \text{KG}_j(x_i^{base})$  where KG denotes the knowledge graph, and  $j = 1, \dots, N$ .

**Enhancing commonsense knowledge rule with LLM.** After obtaining the basic commonsense knowledge, we use GPT-3.5 (Ouyang et al., 2022) to introduce rich context descriptions. This is because even after introducing related entities via ConceptNet relations, these commonsense knowledge descriptions based on our templates remain too brief. The expansion by GPT-3.5 allows for an enhanced expression of this common sense knowledge with higher quality vocabulary, syntax, semantic coherence, etc. Furthermore, as GPT-3.5 is a model pretrained with a vast amount of knowledge, it can also further supplement the knowledge in its generation, leading to descriptions with richer details (see examples in Figure 1 green texts).

Concretely, denote the LLM (e.g., GPT-3.5) as  $L$ . For each ConceptNet knowledge  $x_{i,j}^{kg}, j \in [N]$  in each class  $c_i$ , we prompt LLM with “Rewrite the sentence to make the description more detailed: { $x_{i,j}^{kg}$ }” to expand and supplement the sentences. We obtain  $x_{i,j}^l = L(x_{i,j}^{kg})$  as LLM expansion output.

**Retrieval Augmented Generation based on Wikipedia.** We find that LLM-enhanced descriptions still lack sufficient details about the class object and could contain hallucinated content. Therefore, we utilize Retrieval Augmented Generation based on Wikipedia (Wikipedia, 2004), a reliable knowledge store commonly used to fetch factual knowledge, so as to add sufficient details about features of the object. For instance, the pure class name “tench” lacks descriptions of its physical features, while the explicit knowledge from Wikipedia can supplement it (see examples in Figure 1 blue texts).

In particular, we employ ColBERT (Khattab & Zaharia, 2020) for retrieval from a text corpus based on their pre-built Wikipedia index and obtain related information given the query (Semnani et al., 2023). To select related passages, a retrieval model employs an encoder function that projects texts into an embedding space, and then identifies passages that closely resemble the query instance. In essence, the retrieval function assesses the similarity between two textual instances within this embedding space. Following this, a K-Nearest Neighbors (KNN) approach is utilized to identify the most similar passages with high embedding similarity. Formally, let RAG be the retrieval model. For each LLM expanded description  $x_{i,j}^l$  for each class  $c_i$ , we retrieve top  $N_{rag}$  relevant passages from Wikipedia knowledge store through RAG, which are denoted as  $p_{i,j,k}^{rag} = \text{RAG}_k(x_{i,j}^l), k = 1, \dots, N_{rag}$ .



### 3.2 DESCRIPTION SUMMARIZATION AND REFINEMENT

For each class  $c_i$ , given each LLM expanded commonsense description  $\{x_{i,j}^l\}$  and each relevant detailed knowledge description  $\{p_{i,j,k}^{rag}\}$  retrieved from Wikipedia, we use the in-context learning capabilities of GPT-3.5 to summarize these passages and refine the existing knowledge.

Specifically, we use prompt template “*Context:  $\{p_{i,j,k}^{rag}\}$ ; Prompt\_input:  $\{x_{i,j}^l\}$ ; Prompt\_output:*” to combine the knowledge from Wikipedia passages and LLM-expanded descriptions together, and induce the GPT-3.5 to provide summarization and refinement. Moreover, given the in-context learning ability of recent LLMs, we provide *few-shot demonstrations* to improve the generation quality. In particular, we add two polished demonstrations containing LLM-expanded description and Wikipedia passages as input, as well as a concrete polished output displayed after “*Prompt\_output:*”. With those polished demonstrations, denoted as  $d$ , GPT-3.5 tends to perform better, as they help prevent the model from generating irrelevant information. Examples of such manually optimized demonstrations can be found in Appendix D. The final summarized and refined descriptions for each class  $c_i$  are denoted as  $x_{i,j,k}^d = \mathbb{L}(d, x_{i,j}^l, p_{i,j,k}^{rag})$  where  $j \in [N], k \in [N_{rag}]$ .

### 3.3 IMAGE GENERATION WITH CONTROLLED DIVERSITY

In this section, we use the final knowledge-enhanced class descriptions  $\{x_{i,j,k}^d\}$  as the prompts for text-to-image diffusion model to generate diverse images.

**Image generation with enhanced diversity.** We use diffusion model D, such as Stable Diffusion (Rombach et al., 2022), GLIDE (Nichol & Dhariwal, 2021), and DALLE-3 (Betker et al., 2023), to generate  $N_m$  images  $m_{i,j,k,q} = D_q(x_{i,j,k}^d)$  for each prompt  $x_{i,j,k}^d$ , where  $q \in [N_m]$ .

To increase image diversity, we alter the parameter “guidance scale” (Rombach et al., 2022) in the diffusion pipeline to control the balance between the precision of the generated image matching the provided prompt and the generation diversity. Since knowledge-enabled prompts already possess a considerable degree of diversity, and too much diversity could lead to noisy generation and hurt performance (Fan et al., 2023), we do not employ additional methods to increase image diversity. In fact, Shipard et al. (2023) suggests additional tricks for improving synthetic diversity, such as generating stylized images. As their initial prompts are not good, they rely on more image generation tricks to improve diversity. However, in our experiments, we found that adding more tricks is not effective. For example, incorporating stylized images doubles the training dataset size, but the accuracy does not significantly improve and rather decreases in some datasets (see Appendix E).

**Selecting high-quality images.** It is unavoidable that some extracted knowledge texts may not be relevant to the targeted class, or some generated images may be of poor quality. Here, we utilize the CLIP score (Radford et al., 2021) to filter out low-quality images. More specifically, for each generated image  $m_{i,j,k,q}$ , we use the CLIP text embedding  $x_i^{temp}$  for the corresponding class name  $c_i$ , where  $x_i^{temp}$  denote the OpenAI suggested prompt templates for CLIP zero-shot classification.<sup>1</sup> Then, we calculate its cosine similarity with the image embeddings as CLIP score. We filter out images with low scores and obtain the filtered images for fine-tuning:  $\{m_{i,j,k,q} | \cos(\text{CLIP}(m_{i,j,k,q}), \text{CLIP}(x_i^{temp})) \geq \theta\}$ , where CLIP denotes the CLIP encoder for extracting text or image embedding, and  $\theta$  is the threshold.

It is worth noting that our primary goal in using CLIP scores is not to *perform precise quality ranking, but rather to eliminate obviously mismatched samples or failed generations for the targeted class*. We observed that this filtering successfully removes two major types of low-quality samples. (1) *Inadequate Text Refinement*: GPT-3.5 occasionally fails to enhance the ConceptNet relations( Section 3.1) due to errors in the knowledge text. This leads to responses like "This sentence is incorrect and does not make sense", resulting in ineffective prompts and unusable synthetic images. (2) *Failed Synthetic Image Generation*: Due to the randomness of diffusion model generation, synthetic images sometimes fail to meet the specific dataset requirements. For example, synthetic images in the EuroSAT dataset did not resemble actual satellite images. We provide examples of such failure cases on ImageNet (Figure 4) and Eurosat (Figure 5) in Appendix F.

<sup>1</sup><https://github.com/openai/CLIP/blob/main/data/prompts.md>

### 3.4 DOWNSTREAM MODEL FINE-TUNING

We apply the knowledge-enabled synthetic data to improve downstream tasks. Notably, as no original training data is used in our framework, our evaluation belongs to the *zero-shot setting*, demonstrating the versatility applicability of KnowData that only relies on the targeted class names.

**Zero-shot image classification setup.** We focus on improving CLIP models on downstream tasks, given the wide adoption of CLIP for multimodal learning. Considering the potential label space mismatch between CLIP pre-training and the zero-shot downstream task, fine-tuning pretrained CLIP models on our knowledge-enabled dataset can enhance the capabilities.

**Fine-tuning method.** Prior work suggests that finetuning a classifier head based on the frozen pre-trained encoders is sufficient to adapt CLIP to a new task (Wortsman et al., 2022; He et al., 2023). However, in our experiments, we find that we achieve better results by fine-tuning part of the pre-trained image encoder parameters in addition to the classification head. In fact, we believe that knowledge-enhanced data contains more information compared to other baseline synthetic data, and merely fine-tuning the classification head is insufficient for the model to fully learn this content. Therefore, more parameters must be unlocked for the model to learn the distribution. We believe that with the increase in the amount of knowledge-enhanced synthetic data and the richness and accuracy of the knowledge in the data, we will eventually be able to fine-tune the entire pre-trained encoder with better results, which we leave for future work.

## 4 EXPERIMENT

### 4.1 SETUPS

**Datasets.** We use nine datasets, covering object-level, fine-grained, and robustness for zero-shot image classification. (1) *Object-level* includes: (a) Cifar100 (Krizhevsky et al., 2009): extension of the CIFAR-10 dataset to 100 classes, containing low-resolution images. (b) ImageNet (Deng et al., 2009): a large-scale dataset designed for use in visual object recognition software research, containing high-resolution images (abbreviated as ‘IN-Val’). (2) *Fine-grained* includes: (a) DTD (Cimpoi et al., 2014): a collection of textural images in the wild. (b) Eurosat (Helber et al., 2019): a collection of satellite images covering 13 spectral bands and consisting of 10 classes. (3) *Robustness* includes: (a) ImageNet-V2 (Recht et al., 2019): a reproduction of the ImageNet with distribution shift (abbreviated as ‘IN-V2’). (b) ImageNet-Sketch (Wang et al., 2019): black and white sketches of ImageNet (abbreviated as ‘IN-Sketch’). (c) ImageNet-R (Hendrycks et al., 2021a): renditions (e.g., art, patterns, etc.) of 200 ImageNet classes (abbreviated as ‘IN-R’). (d) ObjectNet (Barbu et al., 2019): real-world objects from ImageNet with diversity. (e) ImageNet-A (Hendrycks et al., 2021b): ImageNet with naturally occurring examples filtered (abbreviated as ‘IN-A’).

**Models.** We use GPT-3.5 (Brown et al., 2020) for generating and summarizing knowledge descriptions. By default, we employ the Stable Diffusion (stable-diffusion-v1-5 endpoint) (Rombach et al., 2022) for image generation, and we additionally evaluate GLIDE (Nichol & Dhariwal, 2021) and DALLE-3 (Azure OpenAI API) (Betker et al., 2023) in ablation studies. For fine-tuning on the synthetic data for zero-shot classification, we use two pre-trained CLIP models: CLIP-RN50 based on ResNet-50 (He et al., 2016) and CLIP-ViT-B/16 based on ViT-B/16 (Dosovitskiy et al., 2020). We fine-tune these models using cross-entropy loss, with a learning rate of 1e-5, a weight decay of 0.1, and for 15 epochs. Specifically, we fine-tune the last 31 layers for CLIP-ViT-B/16 and the last 44 layers for CLIP-RN50 (details on selecting the layers to fine-tune are provided in Appendix G.)

**Synthetic dataset details.** We generate 480k synthetic images based on ImageNet class names to fine-tune the downstream models, and then evaluate the fine-tuned models on the ImageNet test data and its out-of-distribution variants. We generate about 60k images for other datasets with fewer categories, including CIFAR100, DTD, and EuroSAT. The detailed number of synthetic prompts and images corresponding to each stage in our pipeline for different datasets can be found in Table 1. We use 10 NVIDIA RTX A6000 to perform data generation. Generating 60k data requires 12 hours.

**Baselines.** We consider the OpenAI’s pretrained CLIP models and 5 state-of-the-art CLIP zero-shot methods in the two categories discussed in Section 2 as our baselines. Specifically, (1) *among baselines that enhance the initial text embeddings*, we evaluate: (a) ZPE (Allingham et al., 2023), which establishes a pool of templates and then improves zero-shot results by using weighted selection

Table 1: Synthetic dataset size at different stages in KnowData.

| Dataset          | # class | # prompts           |                     |                     |                         | # images                  |                            |
|------------------|---------|---------------------|---------------------|---------------------|-------------------------|---------------------------|----------------------------|
|                  |         | after ConceptNet    | after GPT expansion | after Wiki RAG      | after GPT summarization | diffusion model generated | after CLIP score filtering |
| CIFAR100         | 100     | 100 × 100 = 10000   | 10000               | 2 × 10000 = 20000   | 20000                   | 4 × 20000 = 80000         | 0.75 × 80000 = 60000       |
| DTD              | 47      | 100 × 47 = 4700     | 4700                | 2 × 4700 = 9400     | 9400                    | 8 × 9400 = 75200          | 0.8 × 75200 = 60160        |
| EuroSAT          | 10      | 100 × 10 = 1000     | 1000                | 3 × 1000 = 3000     | 3000                    | 25 × 3000 = 75000         | 0.8 × 75000 = 60000        |
| ImageNet&Variant | 1000    | 100 × 1000 = 100000 | 100000              | 2 × 100000 = 200000 | 200000                  | 4 × 200000 = 800000       | 0.6 × 800000 = 480000      |

Table 2: Zero-shot image classification results based on KnowData compared with SOTA methods. The column **S** indicates the use of synthetic data, **P** denotes the use of pre-trained models, **E** represents the incorporation of external knowledge, and **IN-Avg** is the average accuracy across ImageNet and its variants. \* denotes our reproduced results for baselines, and - means that the baseline method does not support the evaluation setting. The highest accuracy across all methods is **bolded**<sup>3</sup>.

| Model                            | Method                               | S | P | E            | CIFAR100     | DTD          | EuroSAT      | IN-Val       | IN-V2        | IN-R   | IN-A          | IN-Sketch    | IN-Avg |
|----------------------------------|--------------------------------------|---|---|--------------|--------------|--------------|--------------|--------------|--------------|--------|---------------|--------------|--------|
| CLIP ViT-B/16                    | OpenAI (Radford et al., 2021)        | × | ✓ | ×            | 68.70        | 46.00        | 54.10        | 68.60        | 61.60*       | 77.57* | <b>50.23*</b> | 48.23*       | 61.25  |
|                                  | ZPE (Alingham et al., 2023)          | × | ✓ | ✓            | 66.63        | 46.28        | 53.82        | 68.60        | 62.21        | 77.62  | 49.63         | 47.99        | 61.21  |
|                                  | Description (Menon & Vondrick, 2023) | × | ✓ | ✓            | -            | 45.59        | 48.82        | 68.03        | 61.54        | 75.00* | 49.17*        | 47.08*       | 60.16  |
|                                  | Hierarchy (Ge et al., 2023)          | × | ✓ | ✓            | 35.20        | -            | -            | 68.86        | 62.00        | 60.62  | 31.07         | 48.26        | 54.16  |
|                                  | Synthetic (He et al., 2023)          | ✓ | ✓ | ✓            | 70.71        | 44.92        | 59.86        | 69.16        | 61.28*       | 76.41  | 48.25*        | 48.47        | 60.71  |
| Diversity (Shipard et al., 2023) | ✓                                    | × | × | 32.38        | -            | 21.71        | -            | -            | -            | -      | -             | -            |        |
| KnowData (ours)                  | ✓                                    | ✓ | ✓ | <b>73.88</b> | <b>57.51</b> | <b>63.86</b> | <b>70.44</b> | <b>64.13</b> | <b>78.20</b> | 48.65  | <b>50.63</b>  | <b>62.41</b> |        |
| CLIP RN50                        | OpenAI (Radford et al., 2021)        | × | ✓ | ×            | 41.60        | 41.70        | 41.10        | 59.60        | 52.92*       | 60.53* | 22.80*        | 35.38*       | 46.25  |
|                                  | Description (Menon & Vondrick, 2023) | × | ✓ | ✓            | -            | 41.90*       | 37.58*       | 59.59*       | 53.02*       | 57.20* | <b>23.55*</b> | 33.73*       | 45.42  |
|                                  | Hierarchy (Ge et al., 2023)          | × | ✓ | ✓            | -            | -            | -            | 59.76*       | 53.11*       | 42.59* | 11.21*        | 35.55*       | 40.44  |
|                                  | Synthetic (He et al., 2023)          | ✓ | ✓ | ✓            | 45.69        | 43.19        | 55.37        | 60.78        | 51.14*       | 59.37  | 21.91*        | 36.55        | 45.95  |
|                                  | Diversity (Shipard et al., 2023)     | ✓ | × | ×            | 45.63        | -            | 39.92        | -            | -            | -      | -             | -            | -      |
| KnowData (ours)                  | ✓                                    | ✓ | ✓ | <b>57.16</b> | <b>51.18</b> | <b>57.19</b> | <b>61.73</b> | <b>54.67</b> | <b>60.67</b> | 19.75  | <b>37.74</b>  | <b>46.91</b> |        |

among these templates to serve as the classification head. (b) **Description** (Menon & Vondrick, 2023), which uses the description of the label instead of the label name itself as the input for text embedding for classification. (c) **Hierarchy** (Ge et al., 2023), which enhances labels through the WordNet hierarchy for data with low confidence. (2) *Among baselines that involve fine-tuning with synthetic images*, we evaluate: (a) **Synthetic** (He et al., 2023), which enhances labels with the T5 model, generates images using these enhanced labels with the GLIDE model and then fine-tunes only the classification head of CLIP. (b) **Diversity** (Shipard et al., 2023), which utilizes images generated with three different tricks to enhance diversity and fine-tunes a model with random initialization.

**Evaluation metrics.** We use three common metrics to evaluate the quality of our generated images. (1) *Accuracy.* For a test image, we input it into the image encoder to get the image embedding. By multiplying this with the classification head and taking the argmax, we can predict the label for the image. The top-1 accuracy across all images is used to determine the final accuracy. (2) *CLIP score.* Unlike the CLIP score used for filtering in Section 3.3, the text embeddings for the CLIP score here are obtained from our knowledge-enabled prompts, rather than being derived from class names combined with each dataset’s CLIP template. This metric reflects the reliability of the generated image regarding the prompt. (3) *Diversity score.* Following Boutin et al. (2023), we compute the standard deviation in the feature space (SimCLR image encoder (Chen et al., 2020)) for images from every class, and then compute the average score across all classes as the diversity score. Specifically, for a given category  $j$ , composed of  $M$  samples and a feature space  $f$ , the diversity  $\sigma_j$  is computed as follows:  $\sigma_j = \sqrt{\frac{1}{M-1} \sum_{i=1}^M (f(v_i^j) - \frac{1}{M} \sum_{i=1}^M f(v_i^j))^2}$ , where  $v_i^j$  is  $i$ -the image of class  $j$ .

## 4.2 EXPERIMENTAL RESULTS

**KnowData improves CLIP’s zero-shot performance.** We evaluate KnowData on zero-shot image classification tasks by fine-tuning CLIP ViT-B/16 and CLIP RN50 models on our generated synthetic data. (1) The results in Table 2 show that, on ViT-B, compared to the best SOTA methods, KnowData achieves 11.23% and 4% performance improvements on the DTD and EuroSAT datasets, respectively. On RN50, the performance improvements were 11.47% and 7.99% on the Cifar100 and DTD datasets, respectively. (2) Besides significant improvements on fine-grained datasets, our results on the ImageNet and its variants consistently surpassed those of SOTA methods. For example, on In-Val dataset with CLIP ViT-B/16 model, the previous SOTA method, Synthetic (He et al., 2023), only achieves 0.56% accuracy improvement over OpenAI CLIP baseline, whereas KnowData reached 1.28% accuracy improvement. This demonstrates the effectiveness of our knowledge-enabled data generation pipeline. Moreover, other SOTA methods performed poorly on individual ImageNet variant datasets, failing to exceed the overall performance of OpenAI CLIP, while our model, fine-tuned with the *same* set of synthetic data, showed better performance cross various

ImageNet variant datasets, proving the out-of-distribution robustness of knowledge empowerment in enhancing zero-shot capabilities.

It is noteworthy that, we have reproduced and compared results from various SOTA CLIP zero-shot classification methods, unlike existing works (Allingham et al., 2023; Menon & Vondrick, 2023; Ge et al., 2023; He et al., 2023) that only compare to OpenAI CLIP baseline. Our results set stronger baselines for evaluation and enable a more comprehensive understanding of related research.

**KnowData produces synthetic images with better reliability and diversity.** In addition to the accuracy evaluated above, we further evaluate the CLIP score and diversity score of synthetic images. In particular, we focus on how different components of KnowData that aim to gradually improve the text descriptions, affect the image quality metrics compared to the base prompt (“BP”). In Table 3,

(1) the CLIP score reflects the alignment between the image and text, ensuring that the image accurately represents the content intended by the text. The results in Table 3 show that as knowledge gradually enriches, the CLIP score tends to increase, indicating that knowledge can improve the reliability of synthetic data, enabling it to generate the content intended by the text more accurately. We note that the decrease when we add Wiki RAG knowledge (“+WRAG”) is mainly due to the CLIP text encoder’s inherent limitation of handling inputs within 77 tokens, leading to the truncation of lengthy texts. (2) Furthermore, the diversity score, calculated using the standard deviation in the feature space for images, also increases as knowledge enriches, demonstrating that the addition of knowledge can also serve as a diversity trick, allowing for generating more rich and varied images.

Table 3: The components in KnowData improve the CLIP score and the diversity of synthetic data. **BP**: the baseline using base prompt “A photo of  $\{c_i\}$ ”. The components of KnowData include: **CN**, adding ConceptNet knowledge; **GPT**, adding GPT expansion; **WRAG**, adding RAG based on Wikipedia.

| Method      | CLIP Score    | Diversity    |
|-------------|---------------|--------------|
| BP          | 0.3274        | 31.13        |
| CN          | 0.3409        | 31.93        |
| CN+GPT      | <b>0.3641</b> | 33.73        |
| CN+WRAG+GPT | 0.3513        | <b>37.02</b> |

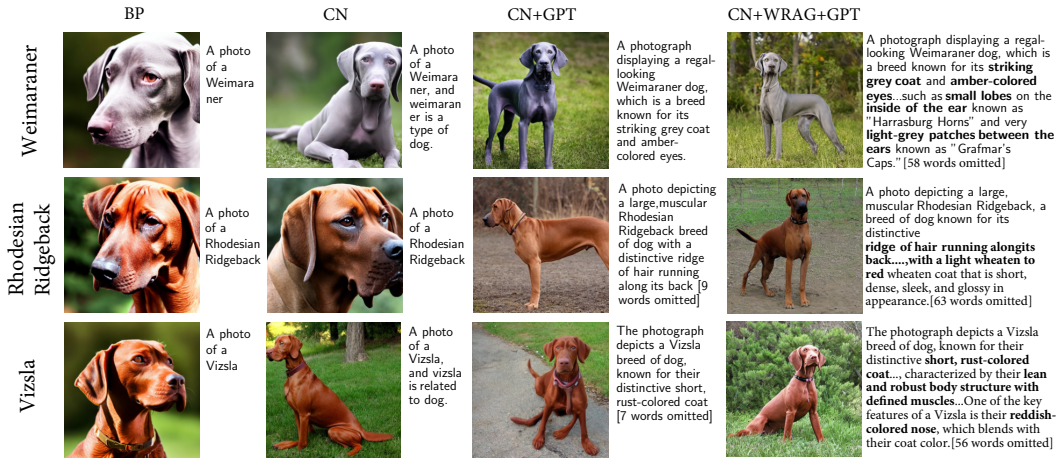


Figure 2: Stable Diffusion generated images for three similar types of dogs (Weimaraner, Rhodesian Ridgeback, Vizsla) given different prompts. KnowData incorporating the knowledge from Concept-Net (CN), GPT-3.5 (GPT) and Wikipedia (WRAG) can generate images of complete objects with better details. However, objects from different classes are less distinguishable under base prompt (BP).

**KnowData produces synthetic images with more accurate details and more diverse background.** In Figure 2 and Appendix Figures 6 to 8, we display pairs of image-text from different numbers of knowledge sources and annotate helpful information in the prompt from each knowledge source. In summary, we find that knowledge-enabled image generation can 1) provide a more complete view

<sup>3</sup>We have filled in the table as much as possible, and reproduced the results for datasets that are not included in the original paper of previous methods to our best. Some dataset/method combinations are difficult to reproduce due to the absence of crucial knowledge or prompts. We mark such cells with “-”.



Table 4: KnowData achieves better results with stronger data generators.

| Data generator   | IN-Val       | IN-V2        | IN-R         | IN-A         | IN-Sketch    | ObjectNet    | Average      |
|------------------|--------------|--------------|--------------|--------------|--------------|--------------|--------------|
| GLIDE            | 67.64        | 61.19        | 76.29        | 47.25        | 48.34        | 51.79        | 58.75        |
| Stable Diffusion | <b>69.85</b> | <b>63.48</b> | 78.16        | <b>49.24</b> | 49.87        | <b>55.10</b> | 60.95        |
| DALLE-3          | 69.66        | 62.93        | <b>78.81</b> | 48.48        | <b>51.47</b> | 54.76        | <b>61.02</b> |

Table 5: Ablation study on diversity in knowledge sources and image generation. **BP**: using base prompt “A photo of  $\{c_i\}$ ”, **CN**: adding ConceptNet knowledge, **GPT**: adding GPT expansion, **Div**: using image diversity tricks, **WRAG**: using RAG based on external knowledge store Wikipedia.

| Model         | Method          | DTD          | EuroSAT      | IN-Val       | IN-V2        | IN-R         | IN-A         | IN-Sketch    | ObjectNet    | Average      |
|---------------|-----------------|--------------|--------------|--------------|--------------|--------------|--------------|--------------|--------------|--------------|
| CLIP ViT-B/16 | BP              | 48.11        | 54.19        | 69.04        | 62.57        | 77.85        | 48.44        | 49.61        | 54.68        | 60.37        |
|               | BP+Div          | 49.17        | 57.90        | 69.64        | 63.03        | 77.88        | 48.08        | 49.80        | 54.93        | 60.56        |
|               | CN+Div          | 53.01        | 60.94        | 69.48        | 62.97        | 77.92        | 48.75        | 49.75        | 54.55        | 60.57        |
|               | PureGPT+Div     | 53.84        | 55.91        | 69.89        | 63.31        | 77.93        | 48.40        | 49.93        | 54.47        | 60.66        |
|               | CN+GPT+Div      | 55.85        | 62.30        | 69.63        | 63.08        | 78.07        | 48.68        | 49.82        | 54.86        | 60.69        |
|               | CN+WRAG+GPT+Div | <b>57.33</b> | <b>63.86</b> | <b>69.95</b> | <b>63.61</b> | <b>78.18</b> | <b>48.81</b> | <b>49.93</b> | <b>55.36</b> | <b>60.97</b> |

of the object, 2) present more accurate details to help differentiate similar classes, and 3) produce more diverse backgrounds. Take Figure 2 with three similar dog species (Weimaraner, Rhodesian Ridgeback, and Vizsla) as an example. We see that with the base prompt, the generated images can distinguish Weimaraner but cannot differentiate between Rhodesian Ridgeback and Vizsla. However, with the addition of knowledge, the generated images can differentiate them through the distinct coat colors (Rhodesian Ridgeback with light wheaten or red wheaten coat, and Vizsla with rust-colored coat) and the unique nose color of Vizsla (reddish-colored nose, which blends with their coat color). Moreover, it is evident that the images generated by the base prompt have a very uniform style of dogs (e.g., showing only the head), while with the addition of knowledge, their poses and backgrounds become increasingly rich and the full body of the dogs are displayed, making the images more realistic.

**KnowData benefits from stronger data generators.** In our experiments, we used open-source Stable Diffusion for synthetic image generation. Here, we study the effect of data generators and additionally evaluate DALLE-3 and GLIDE. We fine-tune CLIP-ViT-B/16 with 60k images generated by different text-to-image generators using KnowData and evaluate the accuracy on ImageNet-Val and its 5 variant testsets. The results in Table 4 show that stronger data generators (Stable Diffusion and DALLE-3 compared to GLIDE) improve zero-shot performance through knowledge-enabled data. It demonstrates the potential of KnowData as the community builds stronger data generators. While both DALLE-3 and Stable Diffusion offer strong performance, we primarily use the open-source model Stable Diffusion in our experiments due to convenience and efficiency.

### KnowData utilizes data more efficiently when scaling synthetic data size.

To study the data scaling law, from the synthetic data filtered by CLIP score (Section 3.3), we randomly sample 10% ~ 100% (in 10% increments) of the data to fine-tune the downstream model. The results on averaged accuracy on ImageNet and its variants (left) and accuracy on DTD dataset (right) in Figure 3 show that KnowData not only surpasses the base prompt method but also shows more noticeable improvement as the volume of data increases, demonstrating better data scaling ability.

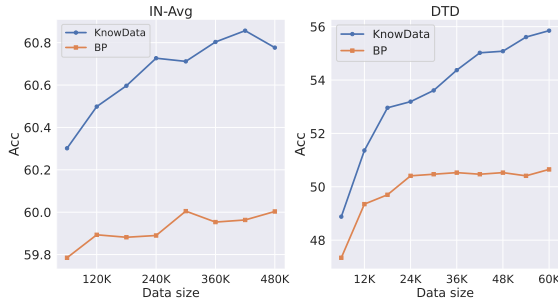


Figure 3: KnowData demonstrates better data scaling law than the base prompt (BP) method in terms of average accuracy on ImageNet (IN-Val and 5 variants) and accuracy on DTD.

**Diversity in knowledge and diversity in images both matter.** In Table 5, we conduct ablation studies on the components of KnowData. Here we fine-tune CLIP-ViT-B/16 with 80k synthetic ImageNet images, and 60k synthetic images for other datasets. (1) From using base prompts (BP), to adding ConceptNet knowledge (+CN), then to incorporating GPT extensions and summaries (+GPT), and finally to adding Wikipedia-based retrieval augmented generation (+WRAG), we see continuous accuracy improvement, underscoring the importance of diverse knowledge sources and text quality in

KnowData. (2) Additionally, the diversity of images is also crucial, as evidenced by the comparison between using and not using diversity techniques (+Div) in the first and second rows. (3) Furthermore, we consider the Pure GPT baseline where we directly prompt GPT-3.5 to generate descriptions about classes (using prompts “write a detailed description about  $\{c_i\}$ ”). The results show that the Pure GPT baseline performs worse than KnowData that incorporates external knowledge sources, including ConceptNet and Wikipedia. It indicates that the descriptions generated by the GPT-3.5 could lack authenticity and diversity due to the potential LLM hallucinations. Explicitly injecting structured knowledge as in KnowData can help improve both accuracy and diversity.

#### KnowData can benefit downstream models with difference sizes.

In addition to CLIP ViT-B/16, we conduct experiments on the larger downstream models such as CLIP ViT-L/14 pretrained on WebImageText (WIT) (Radford et al., 2021) and ViT-G/14 pretrained on LAION-2B (Schuhmann et al., 2022). The results in Table 6 show that the model fine-tuned on KnowData generated synthetic data performs better than pre-trained CLIP (+5.12%) and the SOTA method ZPE (Allingham et al., 2023) (+4.06%) on ViT-L/14, and also surpasses pretrained CLIP (+1.66%) on ViT-G/14<sup>4</sup>. It suggests that even models pre-trained on large datasets with relatively high zero-shot accuracy can still benefit from KnowData’s fine-tuning by a noticeable margin. This indicates that large pre-training datasets might still lack relevant knowledge (e.g., images of certain knowledge might be rare on the internet and thus insufficient in pre-training). KnowData retrieves a comprehensive set of knowledge from ConceptNet, Wikipedia and LLM, and generates corresponding images to supplement the knowledge.

Table 6: Evaluation on different sizes of downstream models.

| Dataset  | Method                        | ViT-B/16     | ViT-L/14     | ViT-G/14     |
|----------|-------------------------------|--------------|--------------|--------------|
| CIFAR100 | OpenAI (Radford et al., 2021) | 68.70        | 78.30        | 83.97        |
|          | ZPE (Allingham et al., 2023)  | 66.63        | 79.36        | -            |
|          | KnowData (ours)               | <b>73.88</b> | <b>83.42</b> | <b>85.70</b> |

#### Fine-tuning CLIP on KnowData improves downstream task performance on VQA and WinoGround.

In addition to image-classification task, KnowData can potentially benefit other downstream tasks. We follow the existing evaluation method (Shen et al., 2021) to evaluate zero-shot performance of CLIP model on VQA v2 dataset (Goyal et al., 2017). Specifically, we append each label used in VQA v2 to the corresponding question in the format  $[Question]+[Label]$  and then calculate zero-shot performance by matching the most similar label to the question’s  $[image]$  embedding. Following (Shen et al., 2021), we evaluate the “yes/no” questions (with question type “Are these...”) on VQA v2 *mini-eval*. We compare the performance of pretrained ViT-B/16 CLIP against the CLIP model finetuned using KnowData synthetic data generated from ImageNet class labels. As shown in Table 7, KnowData-finetuned model can be more generalized with improved accuracy on VQA v2 task.

Table 7: Zero-shot performance of CLIP models on VQA v2 (Goyal et al., 2017) and WinoGround (Thrush et al., 2022) downstream tasks.

| Model                                  | VQA v2       | WinoGround   |              |             |
|--|--------------|--------------|--------------|-------------|
|  | Accuracy     | Text score   | Image score  | Group score |
| Pretrained CLIP (Radford et al., 2021) | 51.62        | 25.25        | 10.25        | 7.00        |
| KnowData-finetuned CLIP                | <b>54.86</b> | <b>27.50</b> | <b>12.00</b> | <b>8.00</b> |

Besides, we evaluate KnowData on WinoGround benchmark (Thrush et al., 2022) which require explicit composition abilities. As shown in Table 7, KnowData fine-tuned CLIP model improves text, image, and group scores. It indicates that the fine-tuned encoders have enhanced composition abilities, allowing them to better discern similar image-text pairs in WinoGround. Given the distinct nature of the knowledge from ImageNet class labels and WinoGround tasks, the results reflect improved generalization capabilities of the fine-tuned model.

## 5 CONCLUSION

In this work, we propose a knowledge-enabled image-text pairs generation framework, KnowData, which leverages real-world knowledge from ConceptNet and Wikipedia, along with large language models and advanced text-to-image models. Our extensive evaluation results show that our approach leads to better CLIP zero-shot performance across various domains, highlighting the importance of integrating diverse knowledge sources for enhancing multimodal learning models.

<sup>4</sup>The result of ZPE on ViT-G/14 is not available in its paper, and ZPE’s implementation is not open-sourced.

## REFERENCES

- 540  
541  
542 James Urquhart Allingham, Jie Ren, Michael W Dusenberry, Xiuye Gu, Yin Cui, Dustin Tran,  
543 Jeremiah Zhe Liu, and Balaji Lakshminarayanan. A simple zero-shot prompt weighting technique  
544 to improve prompt ensembling in text-image models. In *International Conference on Machine*  
545 *Learning*, pp. 547–568. PMLR, 2023.
- 546 Hritik Bansal and Aditya Grover. Leaving reality to imagination: Robust classification via generated  
547 datasets. *arXiv preprint arXiv:2302.02503*, 2023.
- 548 Andrei Barbu, David Mayo, Julian Alverio, William Luo, Christopher Wang, Dan Gutfreund, Josh  
549 Tenenbaum, and Boris Katz. Objectnet: A large-scale bias-controlled dataset for pushing the limits  
550 of object recognition models. *Advances in neural information processing systems*, 32, 2019.
- 551 James Betker, Gabriel Goh, Li Jing, Tim Brooks, Jianfeng Wang, Linjie Li, Long Ouyang, Juntang  
552 Zhuang, Joyce Lee, Yufei Guo, et al. Improving image generation with better captions. *Computer*  
553 *Science*. <https://cdn.openai.com/papers/dall-e-3.pdf>, 2:3, 2023.
- 554 Victor Boutin, Thomas Fel, Lakshya Singhal, Rishav Mukherji, Akash Nagaraj, Julien Colin, and  
555 Thomas Serre. Diffusion models as artists: Are we closing the gap between humans and machines?  
556 *arXiv preprint arXiv:2301.11722*, 2023.
- 557 Tom Brown, Benjamin Mann, Nick Ryder, Melanie Subbiah, Jared D Kaplan, Prafulla Dhariwal,  
558 Arvind Neelakantan, Pranav Shyam, Girish Sastry, Amanda Askell, et al. Language models are  
559 few-shot learners. *Advances in neural information processing systems*, 33:1877–1901, 2020.
- 560 Ting Chen, Simon Kornblith, Mohammad Norouzi, and Geoffrey Hinton. A simple framework for  
561 contrastive learning of visual representations. In *International conference on machine learning*, pp.  
562 1597–1607. PMLR, 2020.
- 563 Mircea Cimpoi, Subhansu Maji, Iasonas Kokkinos, Sammy Mohamed, and Andrea Vedaldi. Describ-  
564 ing textures in the wild. In *Proceedings of the IEEE conference on computer vision and pattern*  
565 *recognition*, pp. 3606–3613, 2014.
- 566 Jia Deng, Wei Dong, Richard Socher, Li-Jia Li, Kai Li, and Li Fei-Fei. Imagenet: A large-scale  
567 hierarchical image database. In *2009 IEEE conference on computer vision and pattern recognition*,  
568 pp. 248–255. Ieee, 2009.
- 569 Alexey Dosovitskiy, Lucas Beyer, Alexander Kolesnikov, Dirk Weissenborn, Xiaohua Zhai, Thomas  
570 Unterthiner, Mostafa Dehghani, Matthias Minderer, Georg Heigold, Sylvain Gelly, et al. An  
571 image is worth 16x16 words: Transformers for image recognition at scale. *arXiv preprint*  
572 *arXiv:2010.11929*, 2020.
- 573 Lijie Fan, Kaifeng Chen, Dilip Krishnan, Dina Katabi, Phillip Isola, and Yonglong Tian. Scaling  
574 laws of synthetic images for model training... for now. *arXiv preprint arXiv:2312.04567*, 2023.
- 575 Alex Fang, Gabriel Ilharco, Mitchell Wortsman, Yuhao Wan, Vaishaal Shankar, Achal Dave, and  
576 Ludwig Schmidt. Data determines distributional robustness in contrastive language image pre-  
577 training (clip). In *International Conference on Machine Learning*, pp. 6216–6234. PMLR, 2022.
- 578 Chen Feng, Georgios Tzimiropoulos, and Ioannis Patras. Clipcleaner: Cleaning noisy labels with clip.  
579 In *Proceedings of the 32nd ACM International Conference on Multimedia*, pp. 876–885, 2024.
- 580 Yunhao Ge, Jie Ren, Andrew Gallagher, Yuxiao Wang, Ming-Hsuan Yang, Hartwig Adam, Laurent Itti,  
581 Balaji Lakshminarayanan, and Jiaping Zhao. Improving zero-shot generalization and robustness  
582 of multi-modal models. In *Proceedings of the IEEE/CVF Conference on Computer Vision and*  
583 *Pattern Recognition*, pp. 11093–11101, 2023.
- 584 Yash Goyal, Tejas Khot, Douglas Summers-Stay, Dhruv Batra, and Devi Parikh. Making the V  
585 in VQA matter: Elevating the role of image understanding in Visual Question Answering. In  
586 *Conference on Computer Vision and Pattern Recognition (CVPR)*, 2017.
- 587 Kaiming He, Xiangyu Zhang, Shaoqing Ren, and Jian Sun. Deep residual learning for image  
588 recognition. In *Proceedings of the IEEE conference on computer vision and pattern recognition*,  
589 pp. 770–778, 2016.

- 594 Ruifei He, Shuyang Sun, Xin Yu, Chuhui Xue, Wenqing Zhang, Philip Torr, Song Bai, and XIAO-  
595 JUAN QI. Is synthetic data from generative models ready for image recognition? In *The Eleventh*  
596 *International Conference on Learning Representations*, 2023.
- 597
- 598 Patrick Helber, Benjamin Bischke, Andreas Dengel, and Damian Borth. Eurosat: A novel dataset  
599 and deep learning benchmark for land use and land cover classification. *IEEE Journal of Selected*  
600 *Topics in Applied Earth Observations and Remote Sensing*, 12(7):2217–2226, 2019.
- 601
- 602 Dan Hendrycks, Steven Basart, Norman Mu, Saurav Kadavath, Frank Wang, Evan Dorundo, Rahul  
603 Desai, Tyler Zhu, Samyak Parajuli, Mike Guo, et al. The many faces of robustness: A critical  
604 analysis of out-of-distribution generalization. In *Proceedings of the IEEE/CVF International*  
605 *Conference on Computer Vision*, pp. 8340–8349, 2021a.
- 606
- 607 Dan Hendrycks, Kevin Zhao, Steven Basart, Jacob Steinhardt, and Dawn Song. Natural adver-  
608 sarial examples. In *Proceedings of the IEEE/CVF Conference on Computer Vision and Pattern*  
609 *Recognition*, pp. 15262–15271, 2021b.
- 610
- 611 Jonathan Ho, Ajay Jain, and Pieter Abbeel. Denoising diffusion probabilistic models. *Advances in*  
612 *neural information processing systems*, 33:6840–6851, 2020.
- 613
- 614 Aidan Hogan, Eva Blomqvist, Michael Cochez, Claudia d’Amato, Gerard De Melo, Claudio Gutierrez,  
615 Sabrina Kirrane, José Emilio Labra Gayo, Roberto Navigli, Sebastian Neumaier, et al. Knowledge  
616 graphs. *ACM Computing Surveys (Csur)*, 54(4):1–37, 2021.
- 617
- 618 Jena D Hwang, Chandra Bhagavatula, Ronan Le Bras, Jeff Da, Keisuke Sakaguchi, Antoine Bosselut,  
619 and Yejin Choi. (comet-) atomic 2020: on symbolic and neural commonsense knowledge graphs.  
620 In *Proceedings of the AAAI Conference on Artificial Intelligence*, volume 35, pp. 6384–6392, 2021.
- 621
- 622 Omar Khattab and Matei Zaharia. Colbert: Efficient and effective passage search via contextualized  
623 late interaction over bert. In *Proceedings of the 43rd International ACM SIGIR conference on*  
624 *research and development in Information Retrieval*, pp. 39–48, 2020.
- 625
- 626 Alex Krizhevsky, Geoffrey Hinton, et al. Learning multiple layers of features from tiny images. 2009.
- 627
- 628 P. Langley. Crafting papers on machine learning. In Pat Langley (ed.), *Proceedings of the 17th*  
629 *International Conference on Machine Learning (ICML 2000)*, pp. 1207–1216, Stanford, CA, 2000.  
630 Morgan Kaufmann.
- 631
- 632 Sachit Menon and Carl Vondrick. Visual classification via description from large language models.  
633 In *The Eleventh International Conference on Learning Representations*, 2023.
- 634
- 635 Thao Nguyen, Gabriel Ilharco, Mitchell Wortsman, Sewoong Oh, and Ludwig Schmidt. Quality not  
636 quantity: On the interaction between dataset design and robustness of clip. *Advances in Neural*  
637 *Information Processing Systems*, 35:21455–21469, 2022.
- 638
- 639 Alexander Quinn Nichol and Prafulla Dhariwal. Improved denoising diffusion probabilistic models.  
640 In *International Conference on Machine Learning*, pp. 8162–8171. PMLR, 2021.
- 641
- 642 Long Ouyang, Jeffrey Wu, Xu Jiang, Diogo Almeida, Carroll Wainwright, Pamela Mishkin, Chong  
643 Zhang, Sandhini Agarwal, Katarina Slama, Alex Ray, et al. Training language models to follow  
644 instructions with human feedback. *Advances in neural information processing systems*, 35:27730–  
645 27744, 2022.
- 646
- 647 Alec Radford, Jong Wook Kim, Chris Hallacy, Aditya Ramesh, Gabriel Goh, Sandhini Agarwal,  
Girish Sastry, Amanda Askell, Pamela Mishkin, Jack Clark, et al. Learning transferable visual  
models from natural language supervision. In *International conference on machine learning*, pp.  
8748–8763. PMLR, 2021.
- Benjamin Recht, Rebecca Roelofs, Ludwig Schmidt, and Vaishaal Shankar. Do imagenet classifiers  
generalize to imagenet? In *International conference on machine learning*, pp. 5389–5400. PMLR,  
2019.



- 648 Robin Rombach, Andreas Blattmann, Dominik Lorenz, Patrick Esser, and Björn Ommer. High-  
649 resolution image synthesis with latent diffusion models. In *Proceedings of the IEEE/CVF confer-*  
650 *ence on computer vision and pattern recognition*, pp. 10684–10695, 2022.
- 651
- 652 Chitwan Saharia, William Chan, Saurabh Saxena, Lala Li, Jay Whang, Emily L Denton, Kamyar  
653 Ghasemipour, Raphael Gontijo Lopes, Burcu Karagol Ayan, Tim Salimans, et al. Photorealistic  
654 text-to-image diffusion models with deep language understanding. *Advances in Neural Information*  
655 *Processing Systems*, 35:36479–36494, 2022.
- 656 Mert Bülent Sariyıldız, Karteek Alahari, Diane Larlus, and Yannis Kalantidis. Fake it till you make  
657 it: Learning transferable representations from synthetic imagenet clones. In *Proceedings of the*  
658 *IEEE/CVF Conference on Computer Vision and Pattern Recognition*, pp. 8011–8021, 2023.
- 659
- 660 Christoph Schuhmann, Romain Beaumont, Richard Vencu, Cade Gordon, Ross Wightman, Mehdi  
661 Cherti, Theo Coombes, Aarush Katta, Clayton Mullis, Mitchell Wortsman, et al. Laion-5b: An  
662 open large-scale dataset for training next generation image-text models. *Advances in Neural*  
663 *Information Processing Systems*, 35:25278–25294, 2022.
- 664 Sina Semnani, Violet Yao, Heidi Zhang, and Monica Lam. Wikichat: Stopping the hallucination of  
665 large language model chatbots by few-shot grounding on wikipedia. In *Findings of the Association*  
666 *for Computational Linguistics: EMNLP 2023*, pp. 2387–2413, 2023.
- 667
- 668 Sheng Shen, Liunian Harold Li, Hao Tan, Mohit Bansal, Anna Rohrbach, Kai-Wei Chang, Zhewei  
669 Yao, and Kurt Keutzer. How much can clip benefit vision-and-language tasks? *arXiv preprint*  
670 *arXiv:2107.06383*, 2021.
- 671
- 672 Jordan Shipard, Arnold Wiliem, Kien Nguyen Thanh, Wei Xiang, and Clinton Fookes. Diversity  
673 is definitely needed: Improving model-agnostic zero-shot classification via stable diffusion. In  
674 *Proceedings of the IEEE/CVF Conference on Computer Vision and Pattern Recognition*, pp.  
675 769–778, 2023.
- 676
- 677 Jascha Sohl-Dickstein, Eric Weiss, Niru Maheswaranathan, and Surya Ganguli. Deep unsupervised  
678 learning using nonequilibrium thermodynamics. In *International conference on machine learning*,  
679 pp. 2256–2265. PMLR, 2015.
- 680
- 681 Robyn Speer, Joshua Chin, and Catherine Havasi. Conceptnet 5.5: An open multilingual graph of  
682 general knowledge. In *Proceedings of the AAAI conference on artificial intelligence*, volume 31,  
683 2017.
- 684
- 685 Tristan Thrush, Ryan Jiang, Max Bartolo, Amanpreet Singh, Adina Williams, Douwe Kiela, and Can-  
686 dace Ross. Winoground: Probing vision and language models for visio-linguistic compositionality.  
687 In *Proceedings of the IEEE/CVF Conference on Computer Vision and Pattern Recognition*, pp.  
688 5238–5248, 2022.
- 689
- 690 Brandon Trabucco, Kyle Doherty, Max Gurinas, and Ruslan Salakhutdinov. Effective data augmenta-  
691 tion with diffusion models. *arXiv preprint arXiv:2302.07944*, 2023.
- 692
- 693 Haohan Wang, Songwei Ge, Zachary Lipton, and Eric P Xing. Learning robust global representations  
694 by penalizing local predictive power. *Advances in Neural Information Processing Systems*, 32,  
695 2019.
- 696
- 697 Wikipedia. Plagiarism — Wikipedia, the free encyclopedia, 2004. URL <http://en.wikipedia.org/w/index.php?title=Plagiarism&oldid=5139350>. [Online; accessed 22-July-  
698 2004].
- 699
- 700 Mitchell Wortsman, Gabriel Ilharco, Jong Wook Kim, Mike Li, Simon Kornblith, Rebecca Roelofs,  
701 Raphael Gontijo Lopes, Hannaneh Hajishirzi, Ali Farhadi, Hongseok Namkoong, et al. Robust  
fine-tuning of zero-shot models. In *Proceedings of the IEEE/CVF Conference on Computer Vision  
and Pattern Recognition*, pp. 7959–7971, 2022.

## 702 A BROADER IMPACT

703  
704 **Positive Societal Impacts** The framework presented in our paper, KnowData, offers several  
705 positive societal impacts, particularly in advancing the capabilities of multimodal models such as  
706 CLIP: (1) *Enhanced Learning and Accessibility*: By integrating real-world knowledge from sources  
707 like knowledge graphs and Wikipedia, KnowData produces more contextually rich and accurate  
708 text descriptions. This can improve the educational value and accessibility of AI-generated content,  
709 making it more informative and beneficial for users. (2) *Improved CLIP Performance*: Our approach  
710 enhances the performance of CLIP models in zero-shot image classification tasks, as demonstrated  
711 by significant performance improvements across multiple datasets. This can lead to more robust  
712 and adaptable CLIP-based systems that perform better in real-world applications. (3) *Promotion of*  
713 *Multimodal Research*: The successful integration of structured and unstructured knowledge into text  
714 descriptions can inspire further research in the integration of diverse data sources for multimodal  
715 learning, fostering innovation and progress in the field.

716 **Negative Societal Impacts and Mitigation Strategies** KnowData integrate real-world knowledge  
717 into text descriptions, thereby enhancing CLIP model performance compared to using purely LLM-  
718 generated text descriptions. While knowledge sources like Wikipedia and ConceptNet are widely  
719 acknowledged as reliable text sources, our framework still relies on LLMs to summarize and refine the  
720 text descriptions. This reliance introduces the possibility that the LLMs may inadvertently introduce  
721 biases or fairness issues affecting certain groups. To mitigate this, future work is needed to research  
722 and apply techniques to detect and reduce biases in the generated content.

## 724 B LIMITATIONS AND FUTURE WORK

725  
726 In our work, we use knowledge-enabled description to generate synthetic images, and use synthetic  
727 images to fine-tune the CLIP models for zero-shot image classification tasks.

728 (1) As discussed in Section 3.4, we found that fine-tuning partial layers of the image encoder performs  
729 better than fine-tuning the entire image encoder. Achieving higher quality image generation, which  
730 might enable effective fine-tuning of the entire image encoder, still requires more comprehensive and  
731 accurate knowledge integration in the future.

732 (2) The fine-tuning process incurs additional computation costs compared to using pretrained CLIP  
733 models. If efficiency is a constraint, the knowledge-enabled texts generated by our KnowData can be  
734 used to directly enhance per-class text embeddings for CLIP image classification without fine-tuning.  
735 We leave the exploration of this approach for future work.

736 (3) Another future work would be comparing our generated text captions with normally collected  
737 ones (e.g., web-crawled image captions). We note that crawling high-quality web image captions and  
738 selecting the most relevant ones for each class label is a challenging and non-trivial task, which could  
739 itself constitute a novel contribution and is a promising future research direction.

740 (4) While our work primarily focuses on evaluating generated synthetic data on downstream image  
741 classification/VQA tasks, extending our evaluation to improve other vision-language capabilities of  
742 CLIP, including text/image retrieval, is an important and exciting direction.

## 745 C CONCEPTNET KNOWLEDGE

746  
747 We focus on 18 relations from ConceptNet: “RelatedTo”, “FormOf”, “IsA”, “PartOf”,  
748 “HasA”, “UsedFor”, “CapableOf”, “AtLocation”, “HasProperty”, “CreatedBy”, “SymbolOf”, “De-  
749 finedAs”, “LocatedNear”, “HasContext”, “SimilarTo”, “MadeOf”, “CausesDesire”, “ReceivesAction”.

750 To convert these relations into more understandable sentences, we use the templates: “{} is related  
751 to {}”, “{} is a form of {}”, “{} is a type of {}”, “{} is a part of {}”, “{} has {}”, “{} is used for  
752 {}”, “{} is capable of {}”, “{} is at the location of {}”, “{} can be described as {}”, “{} is created by  
753 {}”, “{} symbolically represents {}”, “{} and {} overlap considerably in meaning, and {} is a more  
754 explanatory version of {}”, “{} and {} are typically found near each other”, “{} is a word used in the  
755 context of {}”, “{} is similar to {}”, “{} is made of {}”, “{} makes someone want {}”, “{} can be done  
to {}”.

## D IN-CONTEXT LEARNING METHOD FOR RETRIEVAL AUGMENTED GENERATION

We use the following template to guide GPT in summarizing the content of passages retrieved and to adjust and supplement the original prompt.

```
{example0}
{example1}
-----
Context:
{passage_input}
Prompt input:
{prompt_input}
Prompt output:
```

The examples were manually polished by us, totaling 20 in number. For each prompt, we randomly select 2 to be incorporated into the aforementioned template, which, along with the sentence itself and the passage retrieved, guide GPT in the generation process. Here, we showcase two of these examples.

```
-----
Context:
Tincinae Tincinae is a subfamily of freshwater ray-finned fish from the family Cyprinidae, it consists of the tench of Eurasia and the east Asian clod minnows. Tinca tinca is a freshwater tincinae fish that is found in the Danube basin
Prompt input:
A photo of a tench, which is a freshwater fish belonging to the family cyprinidae characterized by its olive-green coloration and small scales.
Prompt output:
A photo of a Tinca tinca, a freshwater tench from the Tincinae subfamily within the Cyprinidae family, characterized by its olive-green coloration and small scales, native to the Danube basin in Eurasia.
```

```
-----
Context:
Goldfish The Goldfish (Carassius auratus) is a freshwater fish in the family Cyprinidae of order Cypriniformes. Goldfish breeds vary greatly in size, body shape, fin configuration, and coloration (various combinations of white, yellow, orange, red, brown, and black are known). Native to China, the goldfish is a relatively small member of the carp family (which also includes the Prussian carp and the crucian carp). It is commonly kept as a pet in indoor aquariums, and is one of the most popular aquarium fish. Goldfish released into the wild have become an invasive pest in parts of North America. It was first selectively bred for color in imperial China more than 1,000 years ago, where several distinct breeds were developed.
Prompt input:
A photograph capturing the image of a small, bright orange goldfish, a freshwater fish species belonging to the family Cyprinidae known for their distinctive scales and long fins.
Prompt output:
A photograph capturing a small, bright orange Carassius auratus, commonly known as a goldfish, a popular freshwater species from the Cyprinidae family, renowned for its distinctive scales and long fins, and a history of over 1,000 years of selective breeding for varied colorations in China.
```

The reason for this approach is that if we use designed prompts to guide GPT in generation, it can lead to the production of some irrelevant information, as in the example below: *“This sentence accurately describes a goldfish.”*

```
Goldfish The Goldfish (Carassius auratus) is a freshwater fish in the family Cyprinidae of order Cypriniformes. Goldfish breeds vary greatly in size, body shape, fin configuration, and coloration (various combinations of white, yellow, orange, red, brown, and black are known). Native to China, the goldfish is a relatively small member of the carp family (which also includes the Prussian carp and the crucian carp). It is commonly kept as a pet in indoor aquariums, and is one of the most popular aquarium fish. Goldfish released into the wild have become an invasive pest in parts of North America. It was first selectively bred for color in imperial China more than 1,000 years ago, where several distinct breeds were developed.
-----
Given the context information above, please extract the most related information for the following sentence:
"A photograph capturing the image of a small, bright orange goldfish, a freshwater fish species belonging to the family Cyprinidae known for their distinctive scales and long fins.";
and please append the extracted information to the end of this sentence to provide more details for this sentence while maintaining its semantic meaning.
```

```
This sentence accurately describes a goldfish, a freshwater fish in the family Cyprinidae known for their distinctive scales and long fins. Goldfish breeds vary greatly in coloration, and some may be bright orange in color. The goldfish is commonly kept as a pet in indoor aquariums and was first selectively bred for color in imperial China over 1,000 years ago. However, goldfish released into the wild have become an invasive pest in parts of North America.
```

## E CONTROLLING THE DEGREE OF IMAGE DIVERSITY

Given the final prompts from KnowData empowered with knowledge through ConceptNet, Wikipedia, and GPT-3.5, we evaluate two image generation methods: (1) **Random guidance scale**: it is achieved by randomly setting the “guidance scale” parameters in the Stable Diffusion pipeline to control the balance between the precision of the generated image matching the provided prompt and the generation diversity. (2) **Stylization** and random guidance scale: we further add stylization to

810 diversify the prompts, which is achieved by adding corresponding style descriptions (such as photo,  
 811 painting, artwork, sketch, collage, poster, digital art image, rock painting, doodle, 3D rendering) to  
 812 the prompt templates, so as to enhance the diversity of image generation. The number of images  
 813 generated for these two methods are 0.6M and 1.2M, respectively.

814 The results in Table 8 show that the accuracy does not increase but decreases despite the doubling in  
 815 the size of the training dataset. To facilitate subsequent testing and achieve better results, we choose  
 816 to use the randomized guidance scale as our method to enhance image diversity.  
 817

819 Table 8: Adding stylization during image generation process does not necessarily improve the  
 820 overall synthetic image quality for ImageNet, as reflected by the zero-shot performance of fine-tuned  
 821 downstream CLIP RN50 models.

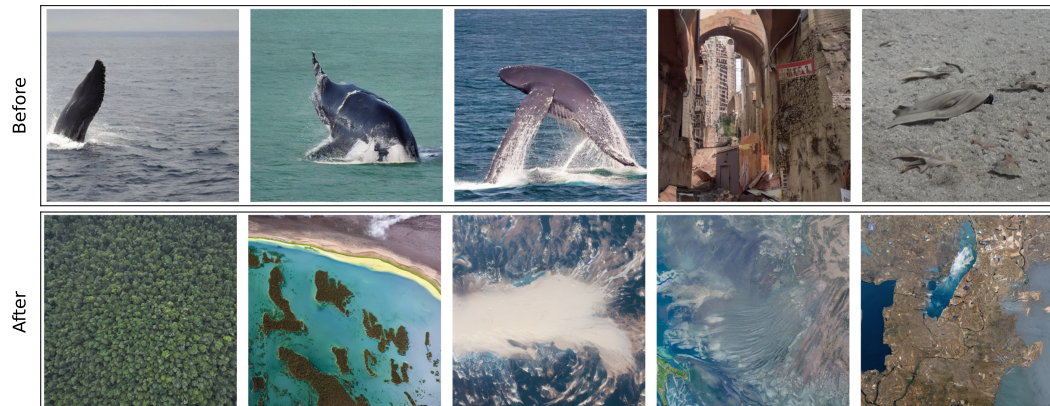
822

| Model     | Method                              | # Synthetic images | IN-Val       | IN-V2        | IN-R         | IN-A         | IN-Sketch    | ObjectNet    |
|-----------|-------------------------------------|--------------------|--------------|--------------|--------------|--------------|--------------|--------------|
| CLIP RN50 | Random guidance scale               | 0.6M               | <b>61.33</b> | <b>54.17</b> | 60.61        | <b>23.04</b> | 35.89        | <b>47.01</b> |
|           | Stylization + Random guidance scale | 1.2M               | 61.10        | 53.89        | <b>60.63</b> | 22.75        | <b>36.00</b> | 46.87        |

826



843 Figure 4: Five images with the lowest CLIP scores from synthetic ImageNet dataset before and after  
 844 applying CLIP score filtering.



862 Figure 5: Five images with the lowest CLIP scores from synthetic EuroSAT dataset before and after  
 863 applying CLIP score filtering.



## F CLIP SCORE FILTERING RESULTS

We present the five images with the lowest CLIP scores from ImageNet (see Figure 4) and EuroSAT (see Figure 5) before and after applying CLIP score filtering. We identify two major failure patterns in low-quality images before filtering: (1) *Inadequate Text Refinement*: GPT-3.5 occasionally fails to enhance the ConceptNet relations( Section 3.1) due to errors in the knowledge text. This leads to responses like "This sentence is incorrect and does not make sense", resulting in ineffective prompts and unusable synthetic images. (2) *Failed Synthetic Image Generation*: Due to the randomness of diffusion model generation, synthetic images sometimes fail to meet the specific dataset requirements. For example, synthetic images in the EuroSAT dataset did not resemble actual satellite images.

After applying CLIP score filtering, images that did not meet the overall dataset requirements (such as the necessary satellite images in EuroSAT) and those generated from inappropriate text descriptions (as in ImageNet) were effectively filtered out. This process significantly improved the quality and relevance of the remaining images.

## G DETAILS ON CLIP MODEL FINE-TUNING

We treat the number of model layers in the pretrained CLIP model to fine-tune as a hyperparameter. Starting from the classification head, we gradually unfreeze more blocks in the image encoders to fine-tune while keeping the remaining layers frozen. As shown in Table 9, the ViT-B/16 model performs best when fine-tuning the last 31 layers (including the classification head) with a 480k ImageNet synthetic dataset. Therefore, we choose to fine-tune the last 31 layers for evaluation on the CIFAR, EuroSAT, and ImageNet variant datasets. Similarly, for the RN50 model, we choose to fine-tune the last 44 layers.

It is noteworthy that although we select the layers to fine-tune based on the results from the ImageNet validation dataset, the evaluation results on other ImageNet variant datasets show that the chosen layers consistently yield better performance across multiple datasets.

Table 9: Performance on IN-Val, IN-V2, IN-R, IN-A, IN-Sketch and ObjectNet when fine-tuning different numbers of layers in pretrained CLIP ViT-B/16 on KnowData generated synthetic ImageNet data.

| Model         | Number of fine-tuning layers | Layers description                           | IN-Val       | IN-V2        | IN-R         | IN-A         | IN-Sketch    | ObjectNet    |
|---------------|------------------------------|--|--------------|--------------|--------------|--------------|--------------|--------------|
| CLIP ViT-B/16 | last 2 layers                | Classification Head                          | 69.64        | 63.01        | 77.83        | <b>50.81</b> | 49.11        | 54.71        |
|               | last 7 layers                | LayerNorm+Classification Head                | 68.98        | 62.15        | 77.44        | 49.51        | 48.22        | 54.20        |
|               | last 19 layers               | 11th Block+LayerNorm+Classification Head     | 70.22        | 63.39        | 77.87        | 49.04        | 49.44        | 54.93        |
|               | last 31 layers               | 10-11th Blocks+LayerNorm+Classification Head | <b>70.41</b> | <b>63.95</b> | 78.25        | 48.84        | 49.70        | <b>55.00</b> |
|               | last 43 layers               | 9-11th Blocks+LayerNorm+Classification Head  | 70.34        | 63.40        | <b>78.49</b> | 48.41        | <b>49.98</b> | 54.87        |
|               | last 55 layers               | 8-11th Blocks+LayerNorm+Classification Head  | 70.15        | 63.04        | 77.58        | 48.00        | 49.70        | 54.22        |

Table 10: Performance on IN-Val, IN-V2, IN-R, IN-A, and IN-Sketch when fine-tuning different numbers of layers in pretrained CLIP RN50 on KnowData generated synthetic ImageNet data.

| Model     | Number of fine-tuning layers | Layers description                             | IN-Val       | IN-V2        | IN-R         | IN-A         | IN-Sketch    |
|-----------|------------------------------|--|--------------|--------------|--------------|--------------|--------------|
| CLIP RN50 | last 2 layers                | Classification Head                            | 60.24        | 53.16        | 60.35        | <b>22.39</b> | 35.35        |
|           | last 44 layers               | 4th Block+AttentionPool+Classification Head    | <b>61.75</b> | 54.44        | <b>60.48</b> | 20.19        | <b>36.85</b> |
|           | last 101 layers              | 3-4th Blocks+AttentionPool+Classification Head | 61.73        | 54.37        | 59.89        | 18.15        | 36.20        |
|           | last 140 layers              | 2-4th Blocks+AttentionPool+Classification Head | 61.55        | <b>54.57</b> | 59.81        | 17.80        | 36.41        |
|           | last 170 layers              | 1-4th Blocks+AttentionPool+Classification Head | 61.58        | 54.42        | 59.80        | 17.88        | 36.34        |

## H EXAMPLES OF KNOWLEDGE-ENABLED GENERATION OF TEXT-IMAGE PAIRS

In Figures 6 to 8, we display pairs of images and their corresponding text generated from varying numbers of knowledge sources. Each prompt is annotated to highlight the helpful information contributed by each knowledge source. We find that knowledge-enabled image generation can: 1)

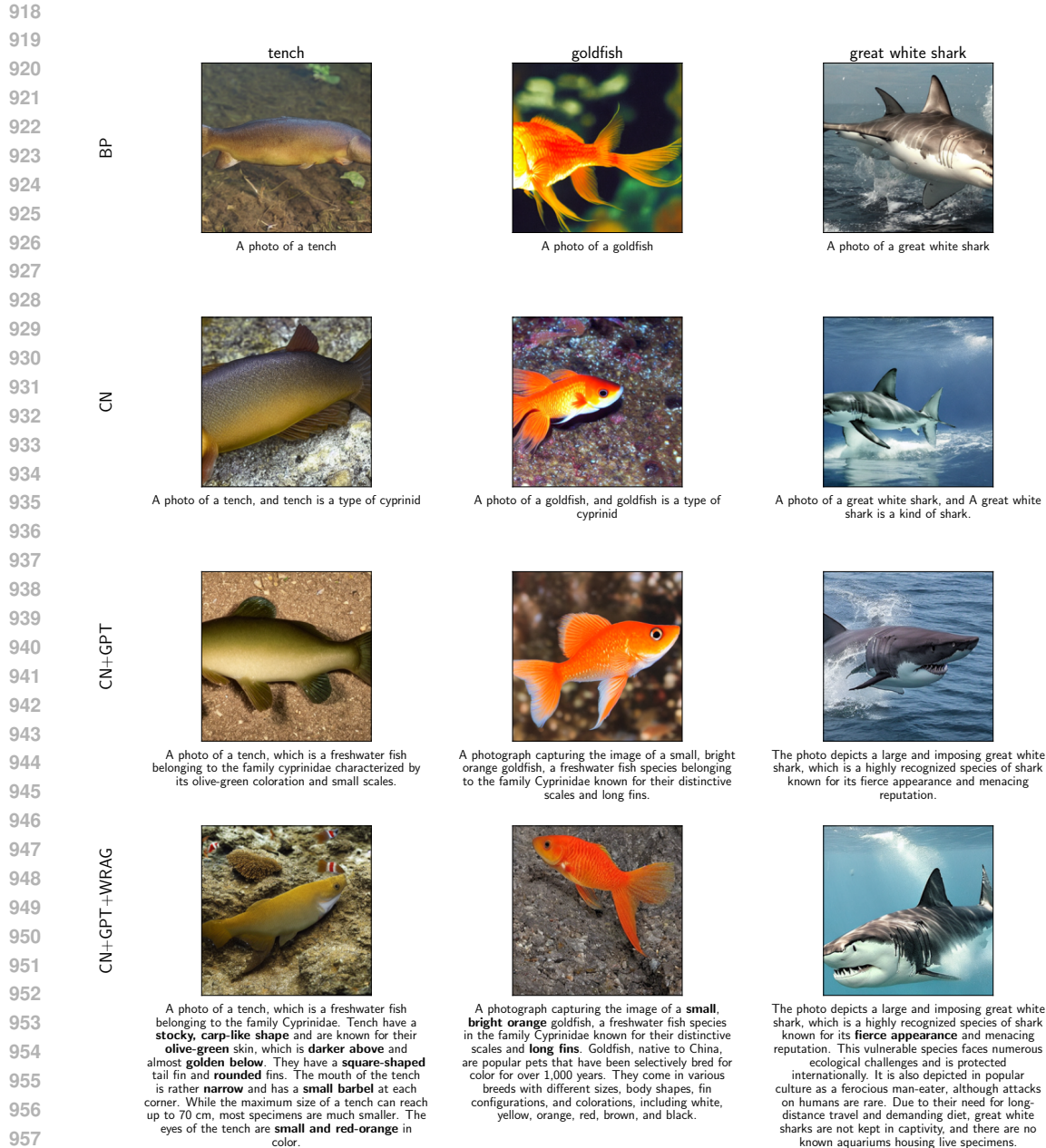


Figure 6: Examples of generated image-text pairs for fish.

Provide a more complete view of the object. 2) Present more accurate details to help differentiate similar classes. 3) Produce more diverse backgrounds.

In the example of fish (Figure 6), it can be seen that fish generated using KnowData can display their complete form, while images generated from the base prompt only show the tail. In the example of birds (Figure 7), it is evident that the background of the KnowData generated images becomes more enriched as knowledge increases. In the example of non-animal objects (Figure 8), additional details can also be seen in KnowData that distinguish between similar types, such as the Acoustic guitar and the Electric guitar. These two types of objects initially have similar backgrounds, but later, the Electric guitar includes an amplifier when Wikipedia knowledge is incorporated.

972  
973  
974  
975  
976  
977  
978  
979  
980  
981  
982  
983  
984  
985  
986  
987  
988  
989  
990  
991  
992  
993  
994  
995  
996  
997  
998  
999  
1000  
1001  
1002  
1003  
1004  
1005  
1006  
1007  
1008  
1009  
1010  
1011  
1012  
1013  
1014  
1015  
1016  
1017  
1018  
1019  
1020  
1021  
1022  
1023  
1024  
1025

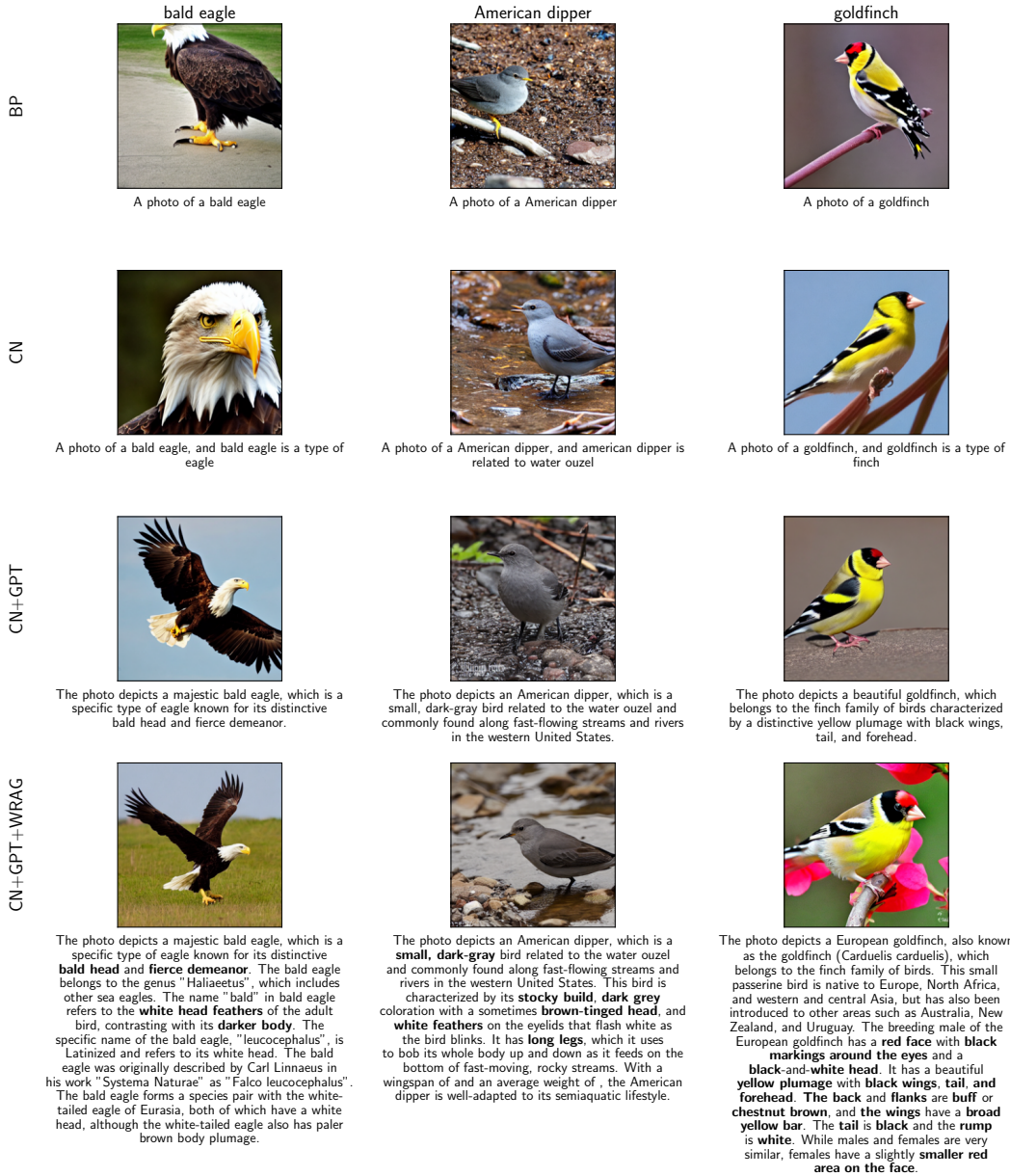


Figure 7: Examples of generated image-text pairs for birds.

1026  
1027  
1028  
1029  
1030  
1031  
1032  
1033  
1034  
1035  
1036  
1037  
1038  
1039  
1040  
1041  
1042  
1043  
1044  
1045  
1046  
1047  
1048  
1049  
1050  
1051  
1052  
1053  
1054  
1055  
1056  
1057  
1058  
1059  
1060  
1061  
1062  
1063  
1064  
1065  
1066  
1067  
1068  
1069  
1070  
1071  
1072  
1073  
1074  
1075  
1076  
1077  
1078  
1079













|             |   |   |  |
|-------------|---|---|--|
| BP          | <p>Acoustic guitar</p>  <p>A photo of a acoustic guitar</p>  | <p>Electric guitar</p>  <p>A photo of a electric guitar</p>  | <p>Violin</p>  <p>A photo of a violin</p>   |
| CN          |  <p>A photo of a acoustic guitar, and acoustic guitar is a type of guitar</p>  |  <p>A photo of a electric guitar, and electric guitar is a type of guitar</p>  |  <p>A photo of a violin</p>   |
| CN+GPT      |  <p>This is a photo of an acoustic guitar, which is a type of guitar with a hollow body that amplifies the sound produced by the strings when they are played.</p>  |  <p>A photograph depicting an electric guitar, which is a musical instrument that is similar to a traditional guitar, but features electronic amplification and pickups that enable it to produce a louder and more versatile sound.</p>  |  <p>A photo depicting a wooden musical instrument with four strings, typically played with a bow across its strings and known as a violin.</p>   |
| CN+GPT+WRAG |  <p>This is a photo of an acoustic guitar, a type of guitar with a <b>hollow body</b> that amplifies the sound produced by the strings when they are played. <b>Unlike electric guitars</b>, acoustic guitars do not rely on electromagnetic pickups or amplifiers to produce sound. Acoustic guitars are commonly used in jazz, blues, R &amp; B, and rock and roll music. They are known for their lower fretboard action, lighter strings, and techniques such as tapping, legato, pinch harmonics, volume swells, and the use of a tremolo arm or effects pedals are less frequently used on acoustic guitars.</p> |  <p>A photograph depicting an electric guitar, which is a musical instrument that is similar to a traditional guitar, but <b>features electronic amplification and pickups</b> that enable it to produce a louder and more versatile sound. Unlike a standard acoustic guitar, an electric guitar requires <b>external amplification</b> to be heard at typical performance volumes. It uses one or more pickups to convert the vibration of its strings into electrical signals, which are then reproduced as sound by loudspeakers. This allows for the shaping and alteration of the sound through various amplifier settings and effects such as reverb and distortion. The electric guitar has played a significant role in the development of multiple genres of music, including jazz, blues, rock and roll, and heavy metal.</p> |  <p>A photo depicting a violin, sometimes referred to as a "fiddle", is a <b>wooden chordophone</b> in the violin family. It is the smallest and highest-pitched instrument in the family and is typically played by drawing a bow across its strings. The violin has a <b>hollow wooden body</b> and usually has <b>four strings</b> tuned in perfect fifths. It can also be played by plucking the strings with the fingers (pizzicato) and by striking the strings with the wooden side of the bow (col legno). Violins are important instruments in a wide variety of musical genres, including Western classical music, folk music, jazz, and even rock music when used with electric amplification.</p> |

Figure 8: Examples of generated image-text pairs for non-animal objects.